Time-domain Fourier optics for polarization-mode dispersion compensation

M. Romagnoli, P. Franco, R. Corsini, and A. Schiffini

Pirelli Cavi e Sistemi S.p.a., viale Sarca 222, 20126 Milan, Italy

M. Midrio

Dipartimento di Ingegneria Elettronica, Gestionale e Meccanica, via delle Scienze 208, 33100 Udine, Italy

Received April 30, 1999

We report on a novel technique to compensate for all-order polarization-mode dispersion. By means of this technique, based on a suitable combination of phase modulation and group-velocity dispersion, we compensated for as much as 60 ps of differential group delay that affected a 10-Gbit/s return-to-zero data stream. © 1999 Optical Society of America

OCIS codes: 060.2330, 060.4510, 260.2030, 070.2580.

One of the major drawbacks of high-bit-rate transmission systems is the presence of random birefringence of the fibers, which leads to polarization-mode dispersion (PMD). New techniques of fiber fabrication allow one to achieve low values of polarization-mode dispersion (PMD), but this does not necessarily hold for the large number of already-installed fibers. For these fibers the value of PMD may increase with respect to that of new fibers, either because of the phenomenon of stress relaxation in aged silica or because of the use of old fabrication techniques. In practice, transfer of the laboratory technology to the field is often limited by this problem. Attempts to envisage PMD-compensation techniques have been carried out.[1–4] Considering that the main difficulty with compensation arises from the time-dependent stochastic nature of PMD, the compensation devices that have been reported are required to continuously feedback the input signal. For this reason these devices have a compensation rate that does not account for relatively fast fiber differential group-delay (DGD) fluctuations. Moreover, second-order PMD is a further issue to be taken into account in the compensation technique. The contribution of second-order PMD becomes increasingly important in high-bit-rate transmission systems.[5] Means of compensating for second-order PMD have been reported,[3] but their practical implementation is quite cumbersome.

The basic idea proposed in this Letter relies on a technique that, independently of the input state of polarization, substantially converts temporal fluctuations into frequency fluctuations. When this technique is used at the receiver, it is possible to restore the signal profile in the temporal domain, leading to a substantial opening of the eye-closure diagram.

To illustrate the basic operation of the device let us assume a return-to-zero (RZ) modulation format, where the single bit 1 is a Gaussian pulse defined as

$$u(0,t) = \exp\left[-\frac{(t-\tau_0)^2}{2{T_0}^2}\right]. \tag{1}$$

The temporal offset τ_0 is a generic displacement that is due to a fluctuation; in the case of PMD we assume that the original pulse is split into two orthogonal components that are equally separated by τ_0 with respect to the center of the time slot. Note, however, that the time $2\tau_0$ has to be less the time-slot duration.

Suppose that we apply a synchronous phase modulation to the incoming signal,

$$m(t) = \exp[i\alpha_m \cos(\Omega_m t)] \approx \exp(iKt^2), \tag{2}$$

which for the sake of simplicity has been expanded around the peak and $K = {}^1\!/_2\,\alpha_m{\Omega_m}^2$. The parameters α_m and Ω_m in Eq. (2) refer to modulation depth and frequency, respectively. After phase modulation we let the signal propagate through a span L of dispersive fiber such that the total group delay at the end is $D = \beta_2 L$, where β_2 is the group-velocity dispersion coefficient. It is possible to demonstrate that

$$KD = -1/2. \tag{3}$$

The combination of phase modulation followed by a dispersive element provides an output signal that is proportional to the Fourier transform of the input, $\tilde{u}(\Omega) = \mathcal{F}[u(t)]$.

The output signal reads as

$$u(L,t) = (2\pi/D)^{1/2}\exp\left[i\left(2K{\tau_0}^2 - \frac{\pi}{4}\right)\right] \times \exp[-i(\Omega_0 t - \phi)]\tilde{u}(0,\Omega), \tag{4}$$

in which the phase factor $\phi = Kt^2$ is the parabolic chirp induced by the phase modulator, where $\Omega_0 = 2K\tau_0$ results in conversion from a temporal offset τ_0 to a spectral offset Ω_0. The frequency offset is also the reason why the device is not readily usable in line. For the specific case of the RZ pulse defined in Eq. (1),

0146-9592/99/171197-03$15.00/0

Eq. (4) becomes

$$u(L,t) = -\sqrt{4\pi}\,T_0 K \exp\left[-i\left(\frac{\pi}{4} + K\tau_0{}^2\right)\right] \times \exp(-iKt^2)\exp(-i\Omega_0 t)\exp(-2K^2T_0{}^2t^2). \quad (5)$$

It is clear from Eq. (5) that the initial pulse displacement τ_0 is exactly compensated for. Moreover, by setting

$$K = 1/2T_0{}^2, \qquad |D| = T_0{}^2 \quad (6)$$

we find that the input pulse width is exactly restored, too.

To provide insight into how the device operates we show in Fig. 1 the case of a split Gaussian pulse, e.g., as a result of the DGD of the fiber link. The splitting of the pulse is equal to $2\tau_0$ and is symmetrical with respect to the reference that we choose in the middle. The phase modulation is parabolic as in Eq. (2). Choosing the condition given by Eq. (3) and the set of parameters given by Eqs. (6), we obtain an exact restoration of the initial pulse condition. To provide a deeper insight into the restoration mechanism we observe that, on the basis of Eq. (4), the restored pulse is exactly the spectrum of the pair of Gaussians shown in Fig. 1, spaced $2\tau_0$ apart. It is particularly interesting that the RZ modulation format is typically composed of Gaussian or hyperbolic secant pulses, which are both invariant under Fourier transformation. That this is so explains the convenience of using the polarization-mode dispersion compensator (PMDC) in combination with the RZ modulation format.

Under real conditions the phase modulation is sinusoidal instead of parabolic as in the ideal situation. To verify the behavior of the PMDC based on sinusoidal modulation and when it is placed at the end of a transmission line we performed numerical simulations by means of a split-step spectral code. The parameters of the simulation were referenced to a 600-km-long transmission line made from six amplified spans of step-index fiber with a loss coefficient of 0.25 dB/km. The dispersion of the fiber was compensated for at each amplification stage with a compensation ratio of 0.9. The data stream at 10 Gbits/s was made of 35-ps-long Gaussian pulses. We set the PMD of the line to 1, 1.16, and 1.25 ps/km$^{1/2}$ to have at the end of the line $\langle$DGD$\rangle$ of 24.5, 28.4, and 30.6 ps, respectively. Considering that the statistical distribution is Maxwellian, we obtain instantaneous values of $(\mathrm{DGD})_{\mathrm{inst}}$ of 73.5, 84.6, and 91.8 ps, i.e., three times the mean values, corresponding to an occurrence probability equal to 10^{-5}. This result is important for transmission systems because, for instance, at a bit rate of 10 Gbits/s a probability of 10^{-5} corresponds to a maximum out-of-service time of 5.2 min per year. The results of the simulations are shown in Fig. 2, in which each data point results from statistics from more than 10^4 random realizations of birefringence of the considered link. Figure 2 displays the complementary probability density as a function of the eye-diagram penalty of the system for the three different values of PMD. Based on the simulation, we show that for the second largest instantaneous value of DGD (84.6 ps) there is a probability of 10^{-4} that the eye closure will be greater than 0.8 dB. The good performance of PMD compensation achieved with sinusoidal phase modulation as an alternative to the ideal case of parabolic phase modulation is indeed verified.

We also performed a laboratory trial to test the PMD penalty reduction that was achieved with the PMDC. The experimental setup is shown in Fig. 3, in which the PMD was simulated with a programmable polarization controller and a variable optical vectorial delay. A 10-GHz repetition-rate source was able to deliver a train of 35-ps-long pulses. The generated train of pulses was sent to a Mach–Zehnder modulator driven by a pattern generator operating at 10 Gbits/s. The data stream was then sent through a polarization controller and a PMD emulator with programmable DGD. The signal affected by instantaneous DGD was sent to the PMDC and then to the detection unit. A detail of the PMDC is shown in Fig. 3(b). The 20-km-long span of step-index fiber

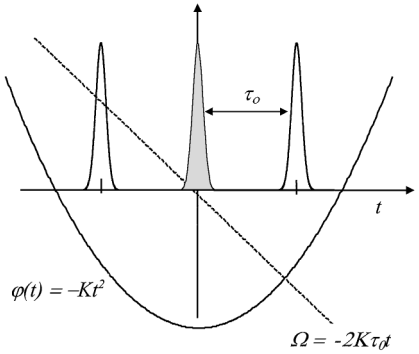

Fig. 1. Diagram of the Fourier transform device. The pair of pulses originally spaced by $2\tau_0$ experiences first a parabolic phase modulation $\varphi(t)$ that induces linear frequency shift and then a dispersion that permits the recombination of the pair at distance $L = -1/(2K\beta_2)$.

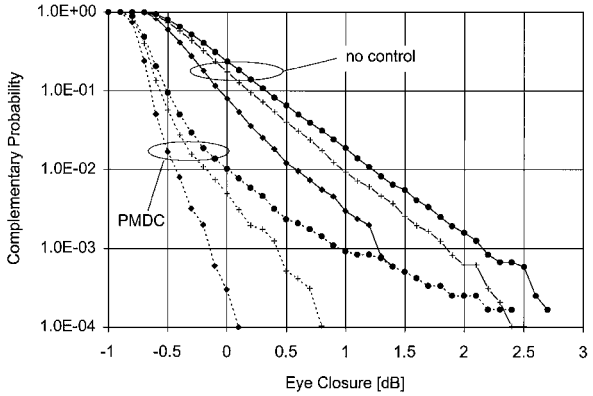

Fig. 2. Probability that the eye-diagram closure results are larger than the corresponding value on the abscissa. The numerical simulation was performed with a RZ signal composed of a 10-Gbit/s stream of 35-ps-long pulses propagating through 6× 100-km spans of step-index fiber with 90% dispersion compensation at each amplification stage. The PMD values (in ps/km$^{1/2}$) are 1 (circles), 1.15 (crosses), and 1.25 (diamonds). The groups of solid and dashed curves refer to the cases without and with the PMDC at the receiver.

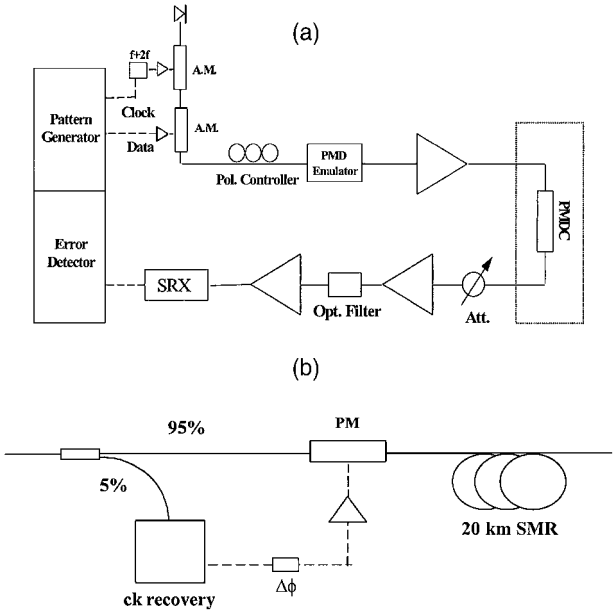

Fig. 3. (a) Experimental setup for the simulation of PMD in a 10-Gbit/s RZ transmission system. A Mach–Zehnder modulator driven by a pattern generator provides a pseudorandom binary sequence 10-Gbit/s stream. To emulate system PMD we send the RZ stream to a programmable polarization (Pol.) controller and then to a DGD device with selectable delay. The emerging signal is sent through the PMDC, the details of which are shown in (b). A.M.'s, amplitude modulators; SRX, receiver; Att., attenuator; SMR, step-index fiber; PM, phase modulator; ck, clock.

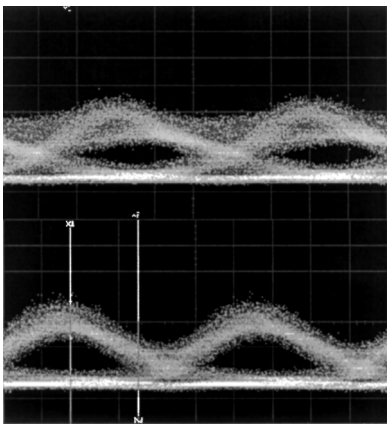

Fig. 4. Eye diagrams of the detected signal affected by 60 ps of DGD: top trace, no PMDC; bottom trace, with PMDC included.

gave a delay $D = -400\ \mathrm{ps}^2$, whereas the modulation amplitude was $\alpha_m = \pi V/V_\pi = 0.7$, thus giving $KD = -0.55$. As an example we show in Fig. 4 eye diagrams measured without and with the PMDC for an input DGD of 60 ps. The performance of the device is shown in Fig. 5. The bit-error rate was measured as a function of the signal-to-noise ratio at the receiver. In Fig. 5 we show two sets of measurements with and without the PMDC. Note that at a bit-error rate of 10^{-9} the penalty as a result

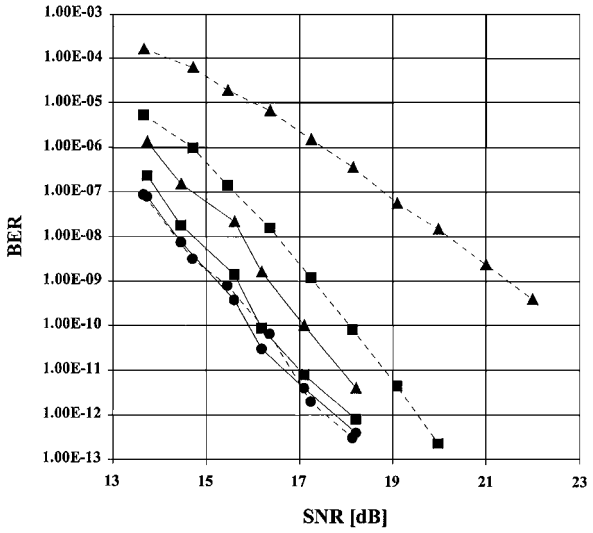

Fig. 5. 10-Gbit/s RZ bit-error rate (BER) measurements. The dashed and solid curves refer to the cases without and with the inclusion of the PMDC, respectively. The values of the programmed delays are DGD's of 0 (circles), 40 ps (squares), and 50 ps (triangles).

of 50 ps of DGD amounted to 6.1 dB, whereas with the PMDC the total penalty was decreased to 1.1 dB.

In conclusion, we have demonstrated that large PMD compensation is achievable with a simple technique that exploits the property of the dispersive propagation of a linearly chirped signal, allowing one to carry out the Fourier transform of the input signal itself. This process, which is intrinsically independent of higher-order PMD, restores each pulse to the center of its own time slot. Moreover, in the experiment done with sinusoidal modulation, i.e., not in the parabolic approximation as in Eq. (1), large operating tolerance was demonstrated.

The authors thank S. Bosso of Pirelli Optical Systems S.p.A. for providing the $LiNbO_3$ devices. M. Romagnoli's e-mail address is marco.romagnoli@pirelli.com.

References

1. F. Heismann, D. A. Fishman, and D. L. Wilson, in *European Conference on Optical Communications (ECOC'98)* (Telefonica de España, Madrid, 1998), pp. 529–530.
2. S. Bigo, G. Bellotti, and M. W. Chbat, in *Digest of Optical Fiber Communication Conference (OFC)* (Optical Society of America, Washington, D.C., 1999), pp. 40–42.
3. C. Glingener, A. Schöpflin, A. Färbert, G. Fisher, R. Noè, D. Sandel, S. Hinz, M. Yoshida-Dierolf, V. Mirvoda, G. Feise, H. Herrmann, R. Ricken, W. Sohler, and F. Wehrmann, in *Optical Fiber Communication Conference (OFC)* (Optical Society of America, Washington, D.C., 1999), postdeadline paper PD-29.
4. H. Bülow, in *Optical Fiber Communication (OFC)* (Optical Society of America, Washington, D.C., 1999), pp. 74–76.
5. P. Ciprut, B. Gisin, N. Gisin, R. Passy, J. P. Von der Weid, F. Prieto, and C. W. Zimmer, J. Lightwave Technol. **16,** 757 (1998).